Received: 1 February 2022 | Revised: 29 June 2022 | Accepted: 1 July 2022

DOI: 10.1002/dvdy.518

RESEARCH ARTICLE

Developmental Dynamics WILEY

Platyfish bypass the constraint of the caudal fin ventral identity in teleosts

Lana Rees | **Désirée König** | **Anna Jaźwińska**

Department of Biology, University of Fribourg, Fribourg, Switzerland

Correspondence
Anna Jaźwińska, Department of Biology, University of Fribourg, Chemin du Musée 10, 1700 Fribourg, Switzerland.
Email: anna.jazwinska@unifr.ch

Funding information
Schweizerischer Nationalfonds zur Förderung der Wissenschaftlichen Forschung; University of Fribourg

Abstract

Background: The caudal fin of teleosts is characterized by dorsoventral symmetry. Despite this external morphology, the principal rays of this appendage connect to bones below the notochord, indicating the ventral (hypochordal) identity of this organ. Results: Here, we report that this typical architecture of the caudal fin is not fully conserved in the platyfish (*Xiphophorus maculatus*) and the guppy (*Poecilia reticulata*), representatives of the *Poeciliidae* family. We show that in these species, 3–4 principal rays connect to bones above the notochord, suggesting an epichordal contribution. Consistently, as examined in platyfish, dorsal identity genes *zic1/4* were highly expressed in these rays, providing molecular evidence of their epichordal origin. Developmental analysis revealed that the earliest rays above the notochord emerge at the 10-ray stage of fin morphogenesis. In contrast to zebrafish and medaka, platyfish and guppies display a mirrored shape of dorsal and ventral processes of the caudal endoskeleton. Our study suggests that an ancestral bauplan expanded in poeciliids by advancing its symmetrical pattern. Conclusion: The platyfish evolved a fin architecture with the epichordal origin of its upper principal rays and a high level of symmetry in the caudal endoskeleton. This innovative architecture highlights the adaptation of the teleost skeleton.

Key findings

1. In platyfish, principal rays of the caudal fin are associated with endoskeletal elements not only below but also above the notochord.
2. Dorsal identity markers *zic1/4* are highly expressed in the three uppermost principal rays.
3. The epichordal principal rays begin to form at the developmental stage with 10 caudal rays.
4. The caudal fin of platyfish displays a striking internal symmetry of the endoskeleton.

KEYWORDS

caudal fin, *Cyprinodontiformes*, developmental morphology, endoskeleton, guppies, hypural plate, medaka, poeciliid, principal rays, Teleosts, *Xiphophorus*, zebrafish, *zic1*, *zic4*

1 | INTRODUCTION

The fins are one the most important innovations of fishes, since these appendages enable efficient locomotion in water. Among them, the caudal fin is particularly important to generate lift, propulsion power and to modulate maneuverability. The dorsoventral symmetry of this appendage has both functional and evolutionary implications.[1-3] Ancestral fishes, possessed an asymmetrical fin, classified as "heterocercal," with a larger dorsal lobe supported by the notochord or vertebral column, and a shorter ventral lobe. In the successive teleosts, the axial skeleton is withdrawn from the appendage, whereas the ancestral ventral lobe gives rise to a symmetrical "homocercal" fin.[2,4-8] From the hydrodynamic perspective, dorsoventrally equilibrated morphology, in which the upper and lower halves are nearly equivalent in area and composition, could advance swimming performance.[9,10] Approximately 96% of extant fish species are teleosts, reflecting the functional benefit of the homocercal tail.

The transition from the heterocercal to homocercal tail was associated with shortening and upward flexion of the notochord.[4,7] Despite this modification and the external fin symmetry, the internal pattern of the associated endoskeleton largely retained its evolutionary origin. As formulated by Sallan, "the teleost caudal fin is actually the ventral lobe of the ancestral fin."[3] Thus, the symmetrical upper and lower fin halves derive from the ventral tissues of the axial skeleton, representing a "hypochordal" (below notochord) identity.[4,5,7,11] Whether some teleost fish could bypass this limitation by increasing the contribution of "epichordal" (above notochord) tissues had not yet been investigated.

The fin comprises an array of exoskeletal elements, called lepidotrichia, which are classified as principal and procurrent rays. According to standard conventions, the principal caudal rays are described as the segmented and branched rays plus one upper and lower unbranched ray located at the lateral margin of each lobe of the fin [6-8,12] (Figure 1A). Briefly, the number of principal rays is defined as the count of branched rays plus two. In practice, the principal rays reach to, or nearly to, the posterior fringe of the fin, whereby their relative length determines the fin shape, which can be forked, truncated or rounded. The procurrent rays are short and serve to widen the base of the fin. Consistent with the phylogenic origin of the homocercal tail, anatomical studies of diverse teleosts have indicated that all the principal rays typically articulate with the hypochordal bones, which are positioned ventrally to the vertebral column, namely hypurals, parhypural and haemal spines. [6-8,12] Thus, with the exception of the dorsal procurrent rays, the principal part of the caudal fin is considered as an organ of ventral origin[3-5] (Figure 1A). This interpretation is consistent with genetic studies in zebrafish,[11] and lineage tracing analysis in medaka that demonstrated a continuous labeling of endoskeletal radials and their associated exoskeletal rays at specific anatomical positions.[13] Based on these results it has been proposed that bones and their attached rays develop from the same population of mesoderm-derived mesenchyme. Thus, the positional identity of rays could to a certain degree be inferred from their attachment to the endoskeleton.

The homocercal tail is considered a beneficial trait for the 250 million years of teleost evolution, given the rich number of more than 30 thousand species.[14,15] Following phylogenic diversifications, certain taxonomic groups evolved unusual characteristics. Among them, the *Poeciliidae* family from the *Cyprinidontiformes* order, displays distinctive features that are rare among fishes.[16,17] Indeed, these fishes do not reproduce by laying eggs, but instead, the fertilization is internal and females carry their offspring for approximately 3 weeks.[18,19] During development, embryos are nourished either from a yolk or through a placenta analog, dependently on species.[20] To achieve the internal fertilization, the anal fin of males is transformed into the gonopodium.[21] In addition, the caudal fin of males may carry secondary sexual traits, such as a ventral sword as seen in swordtails,[22] or as a hypertrophied and elaborately patterned caudal fin, as seen in guppies.[23] Members of the *Poeciliidae* family reveal a particular geographical adaptivity, which is highlighted by the fact that multiple independent populations have colonized habitats with extremely toxic conditions, such as hydrogen sulphide-rich springs in Central America.[24] Thus, poeciliids display a high evolvability potential among teleosts. Whether the developmental symmetry of the caudal endoskeleton was subjected to evolutionary innovation remains yet insufficiently investigated in this group of fish.

A particularly valuable model organism from the *Poeciliidae* family is the platyfish (*Xiphophorus maculatus*). This species has attracted scientific interest for a century thanks to a great variation in pigmentation patterns, sex-

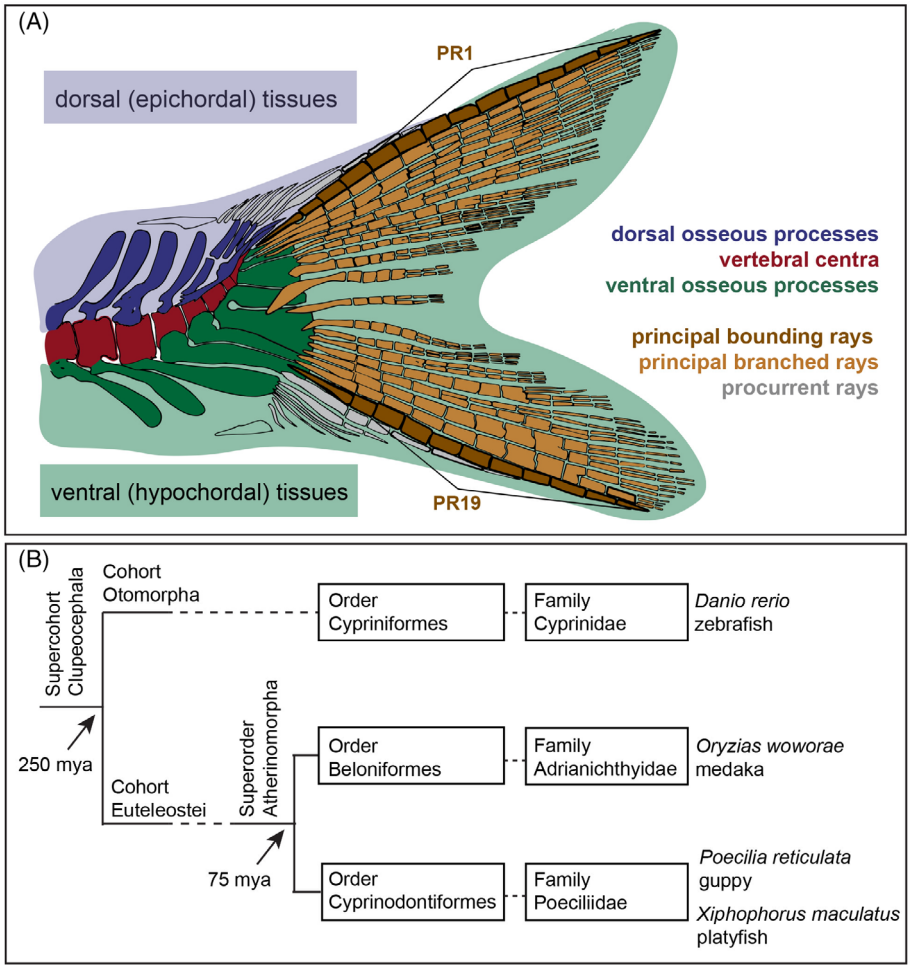

FIGURE 1 The architecture of the homocercal caudal fin and a phylogenic relation of the selected teleost species (A) Fossil reconstruction of homocercal caudal fin of Late Jurassic euteleost *Orthogonikleithrus hoelli*. The caudal fin is supported by principal rays (brown), which include all segmented-and-branched rays framed by one dorsal and one ventral segmented but unbranched ray. The first and last principal rays (PR1 and PR19, dark brown) are the main elements forming the dorsal and ventral leading margins of the caudal fin, respectively. The principal rays articulate with the osseous processes that are situated ventrally to the vertebral centra (red), belonging to the hypochordal (below notochord, green) tissues. The dorsally situated epichordal tissues (purple) support upper procurrent rays (gray) at the base of the fin. The fin is adapted from reference. [7] (B) A simplified phylogenic tree showing the relationships between the 3 species relevant to this study. Arrows indicate the divergence between key branches, according to reference.[15]

reversal ability, susceptibility to melanomas and complex behavior.[25-33] The genome of this species has been sequenced and annotated,[34,35] which renders it suitable for evo-devo research.[36] Given the high evolutionary predisposition to novelties in the *Poeciliidae* family and the use of platyfish in genomic research, we have chosen to investigate whether the caudal skeleton has acquired any distinctive modifications in this species.

To better identify new traits, we compared them with the guppy (*Poecilia reticulata*) from the same *Poeciliidae* family, the *Cyprinodontiformes* order, and with the medaka (*Oryzias woworae*) from a sister order *Beloniformes*[37,38] (Figure 1B). The platyfish and the medaka belong to the same taxonomic monophyletic subseries *Atherinomorpha*, and their last common ancestor existed approximately 75 million years ago.[15,39,40] For comparison, we also included the zebrafish (*Danio rerio*), the most common model fish in biomedical research.[41,42] The platyfish and the zebrafish represent remote phylogenic lineages that separated approximately 220–250 million years ago[15,39,40] (Figure 1B). Besides the anatomical characterization of the adult caudal skeleton, we also analyzed the developmental dynamics of the embryonic tail in platyfish. This morphological and embryological study highlights several unique features, suggesting that the platyfish evolved an exceptional bauplan of the homocercal fin, including epichordal components and an enhanced internal symmetry.

In this study, we attempt to distinguish between the superficial vs anatomical patterns. We use the terms "upper" and "lower" to describe the spatial position relative to the horizontal body axis, whereas "epichordal" and "hypochordal" to define the developmental dorsoventral position relative to the notochord.

2 | RESULTS

2.1 | Comparison of caudal fin rays between platyfish and common model fish species

To characterize the skeleton of the caudal fin, we performed histological staining using Alcian blue & Alizarin red dyes. In two poeciliids, platyfish and guppies, the caudal fin has an oval form with a rounded margin, which

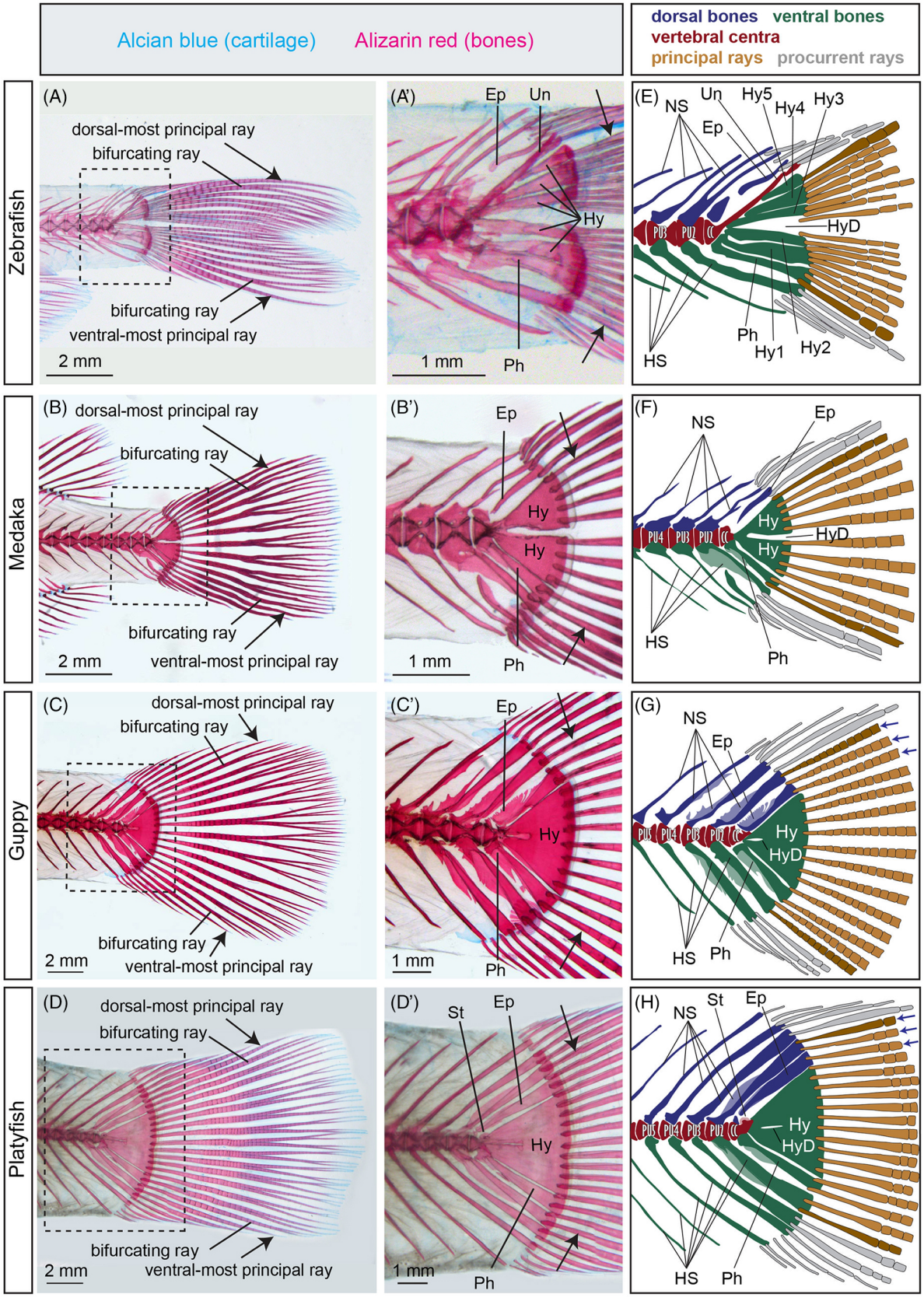

FIGURE 2 Legend on next page.

TABLE 1 Number of rays in the caudal fin of adult platyfish

Specimen	Fin length (mm)	Principal rays	Procurrent rays		Total number of rays
			Upper	Lower	
Male 1	10.38	16	5	9	30
Male 2	10.41	16	6	8	30
Male 3	11.55	17	6	7	30
Male 4	11.84	17	7	6	30
Male 5	11.21	18	5	8	31
Male 6	12.25	18	5	7	30
Female 1	10.97	18	4	6	28
Female 2	10.27	18	5	5	28
Female 3	10.54	18	5	6	29
Female 4	10.61	18	5	7	30
Female 5	10.63	18	5	7	30
Female 6	10.73	18	4	6	28
Average	11.0 ± 0.2	17.5 ± 0.2	5.2 ± 0.2	6.8 ± 0.3	29.5 ± 0.3

Note: The fin length corresponds to the medial longest ray that was measured from the hypural plate to the distal tip on images of Alcian blue and Alizarin red stained specimens. Counting of rays was performed manually. The averages were calculated along with the standard error of the mean (SEM).

contrasts with the forked fin shape of zebrafish and the straight-ended fin of medaka (Figure 2A–D). Examination of 6 male and 6 female platyfish revealed that the maximal length of the caudal fin reached approximately 11 mm, and the fin area was supported by 16–18 principal rays (average 17.5 ± .2; Table 1 and Figure 2D). Then, we counted procurrent rays, which are the short outermost unbranched rays at the dorsal and ventral edge of the appendage. The number of procurrent rays ranged between 4 and 7 (average 5.2 ± 0.2) at the dorsal side, and 5–9 (average 6.8 ± 0.3) at the ventral side (Table 1). We noticed a tendency that the fish with a lower number of principal rays had more procurrent rays, and inversely, so that the total number of all rays ranged from 28 to 31 (average 29.5 ± 0.3).

Interestingly, the zebrafish caudal fin is known to have comparable numbers of 16–19 principal rays and 5–7 procurrent rays at each of dorsal and ventral edges, as reported previously[43-45] (Figure 2A). However, despite nearly the same number of rays, the fin margin displayed opposite geometry, namely, convex (curved outwards) in platyfish vs concave (curved inwards) in zebrafish. This suggests that in these remotely related species, the growth of individual principal rays follows an opposite regulation along the dorso-ventral axis.

In medaka, the distal fin margin has a straight shape, and was supported by 11 principal rays ($N = 6$; 2 females and 4 males) (Figure 2B). The number of procurrent rays ranged between 4 and 5 (average 4.3 ± 0.2) at the dorsal side, and 5–6 (average 5.3 ± 0.2) at the ventral side. Together, the total number of rays was 20–22 (average 20.7 ± 0.4), consistent with a previous study.[46] Thus, although the medaka and the platyfish belong to sister orders (Figure 1B), they show a substantial variation in the number of caudal rays.

FIGURE 2 Comparison of the caudal skeleton in adult zebrafish, medaka and platyfish (A-D) Tails of adult zebrafish (A), medaka (B), guppy (C) and platyfish (D) stained with Alcian blue and Alizarin red to detect cartilage and bone, respectively. The dorsal-most and ventral-most unbranched ray next to a branched ray represents the first and the last principal ray, respectively. The dashed-line frame indicates the area that is magnified in the right panel with the same letter followed by a prime symbol. In the magnified images of the caudal skeleton (A'-D'), the arrows point to the first and the last principal ray. (E-H) Schematic representations of the caudal skeleton based on histological staining. The epichordal (dorsal) bones are in purple, whereas hypochordal (ventral) bones in green. In zebrafish (E) and medaka (F), the principal rays (brown) articulate solely with hypochordal elements. In guppy (G) and platyfish (H), 3 upper principal rays articulate with epichordal bones. Zebrafish $N = 6$; Medaka $N = 6$; Guppy $N = 5$; Platyfish $N = 12$. CC, terminal compound centrum; Ep, epural; Hy, hypural; HyD, hypural diastema; HS, haemal spine; NS, neural spine; Ph, parahypural; PU, preural vertebra numerated from the posterior end; St, stegural (vestigial uroneural), Un, uroneural.

To compare the ray count of platyfish with that of another species from the same *Poeciliidae* family, we analyzed the skeleton of guppies (Figure 2C, C'). We found that in guppies, the number of principal rays ranged between 14 and 16 ($N = 5$), whereas the number of procurrent rays was between 5 and 6 (average 5.4 ± 0.2) at the dorsal side, and 5–7 (average 6.2 ± 0.4) at the ventral side. Thus, *X. maculatus* has a few more principal rays than *P. reticulata*, suggesting variations of the caudal exoskeleton even among these closely related species.

2.2 | Atypical position of dorsal principal rays of the caudal fin in platyfish and guppies

In teleosts, the dorsal-most principal ray is known to align with the dorsal edge of the upper-most hypural, a bone of hypochordal identity (situated below the notochord)[5-8,12]. Consistently, in zebrafish and medaka, the first principal ray articulated with the upper-most hypural (Figure 2A, B, E, F). In platyfish, however, the first principal ray was carried by the neural spine of the preural-2 vertebra (Figure 2D, H). The assessment of 12 platyfish tails demonstrated that 3–4 of the upper principal rays articulated with epichordal bones, namely the epural and neural spines (4 fish with 3 such principal rays; 8 fish with 4 such principal rays). The same anatomical configuration was also observed in guppies (Figure 2C, G). These data demonstrate that the principal caudal fin ray field of poeciliids is not only of ventral origin, but includes a dorsal identity in its upper lobe, which is an atypical situation in teleosts.

Next, we determined the ventral extent of the caudal fin. In zebrafish and medaka, the last principal ray articulates with the haemal spine of the preural-2 vertebra (Figure 2A, B, E, F). A similar anatomical pattern was observed in platyfish and guppies (Figure 2C, D, G, H). Thus, in contrast to the dorsal margin of the principal rays, the ventral bounding remains conserved in all four fish species.

2.3 | Elevated expression of dorsal marker genes *zic1/4* in the 3 uppermost principal rays of the platyfish caudal fin

Genetic studies in medaka suggested that *zic1/4* genes, encoding zinc-finger type transcription factors, are required for the dorsal identity of the mesoderm in the trunk-tail region.[47,48] Thus, the expression level of these two genes could serve to molecularly distinguish between the epichordal vs hypochordal origin of tissues. Accordingly, we identified *zic1/4* orthologues in platyfish and conducted quantitative real-time PCR analysis using cDNA isolated from three parts of the caudal fin; (i) uppermost principal rays 1–3 (upR 1–3), which articulate with the epichordal bones; (ii) upper principal rays 6–8 (upR 6–8), which articulate with the hypural plate; (iii) lower principal rays 1–3 (loR 1–3), which articulate with the haemal spine and parhypural (Figure 3A, B). The latter sample unambiguously comprises tissues of ventral identity, which is predicted to show minimal *zic1/4* expression, and thus, it can be used as calibrator for quantification of relative gene expression. To ensure the reproducibility of results, we performed normalization with two housekeeping genes, *ß-actin 2* (*actb2*) and *polyadenylate-binding protein 1* (*pabp*) in the fin.[49] These qRT-PCR analysis revealed several important results. First, we found that *zic1* and *zic4* transcripts showed approximately 7- to 9-fold increase in the uppermost triplet of principal rays, compared to the lowest triplet (Figure 3C, D). This relatively high *zic1/4* expression in the upper principal rays 1–3 indicates the epichordal origin of this tissue, consistent with our anatomical observation. Second, the intermediate triplet, comprising principal rays 6–8, displayed low *zic1/4* expression that was similar to values detected in the ventral-most principal rays (Figure 3C, D). This result demonstrates that these rays comprise the hypochordal tissue, as predicted from their articulation with the hypural. Third, analysis with both housekeeping genes yielded similar results, namely for *zic1* in upR1-3, we recorded 11.9 and 12.3 normalized gene expression values relative to *actb2* and *pabp*, respectively; for *zic4*, these numbers were 8.8 and 9.2 (Figure 3C, D). These independent quantifications reveal a robust reproducibility of our results. Taken together, we concluded that our qRT-PCR analysis provides a molecular indication for the epichordal origin of the three upper most principal rays in the platyfish caudal fin.

2.4 | Emergence of dorsal caudal rays during platyfish fin morphogenesis

The formation of the caudal skeleton has been well characterized in zebrafish[43,50-53] and medaka.[46,54] This process has not yet been described in platyfish. To understand the dorsal-ventral tissue contribution of the caudal fin in platyfish, we monitored developmental dynamics of ray formation. We dissected embryos from euthanized gravid females at different time-points, and exposed them to calcein, a fluorescent compound that is incorporated by cells at calcification sites, including

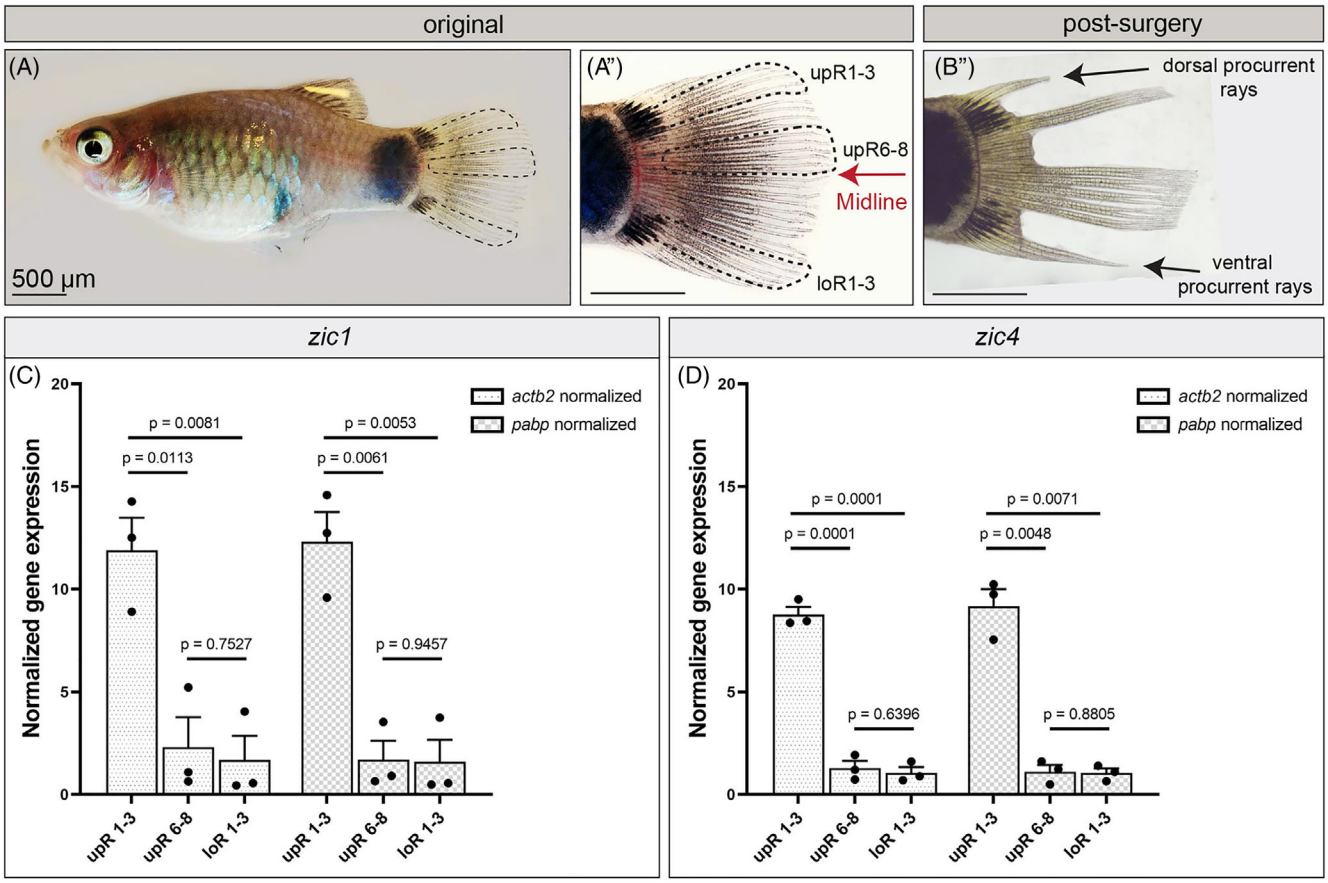

FIGURE 3 The dorsal identity genes *zic1* and *zic4* are highly expressed in the three uppermost principal rays (A) Live imaging of adult platyfish, strain Mickey Mouse Platy. (A') A higher magnification of the caudal tail. Dashed lines encircle triplets of principal rays that were separately collected, a triplet of upper principal rays 1-3 (upR1-3), a triplet of upper principal rays 6-8 above the midline (upR6-8), a triplet of lower principal rays 1-3, counted from the bottom (loR1-3). (B) The same fin as shown to the left after tissue-collection. The notches correspond to the excised tissues. (C, D) qRT-PCR analysis with quantification of *zic1* and *zic4* gene expression normalized to either *actb2* or *pabp* housekeeping genes. $N = 3$ biological replicates, each containing tissues collected from 3 fish. Error bars represent SEM. p values are from unpaired T-test.

rays.[55] We classified the steps of caudal fin morphogenesis by counting rays. To determine the embryo size at each morphogenetic stage, we measured their standard length, defined as the distance from the head tip to the caudal peduncle, as previously established for zebrafish.[56] The correlation between the standard length and the number of caudal rays at different developmental stages was described by a nonlinear regression model ($N = 127$ embryos at different developmental stages; $R^2 = 0.8275$; P-value <0.0001) (Figure 4A). Embryos with the same number of rays varied in size: the highest variation was approximately 10% standard length difference for the group with 25/26 rays. This demonstrates that body growth and organ morphogenesis are not very tightly synchronized during *in-ovario* development, but individual variations are evident among platyfish embryos.

Calcein staining revealed that the earliest pair of rays formed in the middle of the emerging fin, which corresponds to the hypural diastema complex, as described below (Figure 4B). New rays are sequentially added at the upper and lower part of the fin, until the stage with 27/28 rays by the end of embryogenesis. Embryonic caudal fin rays were typically not yet branched, and thus, their prospective principal or procurrent identity cannot be classified during development. This observation is consistent with postembryonic development in zebrafish, showing that ray branching morphogenesis occurs during juvenile growth.[56]

Although calcein intensely stained early developing rays, the caudal endoskeleton became markedly labeled only from the 9/10-ray stage (Figure 4C). This result is consistent with the previous report in zebrafish that endochondral and dermal ray ossification occur independently from each other.[56] At the 9/10-ray stage, two hypural plates were demarcated by calcein at the base of

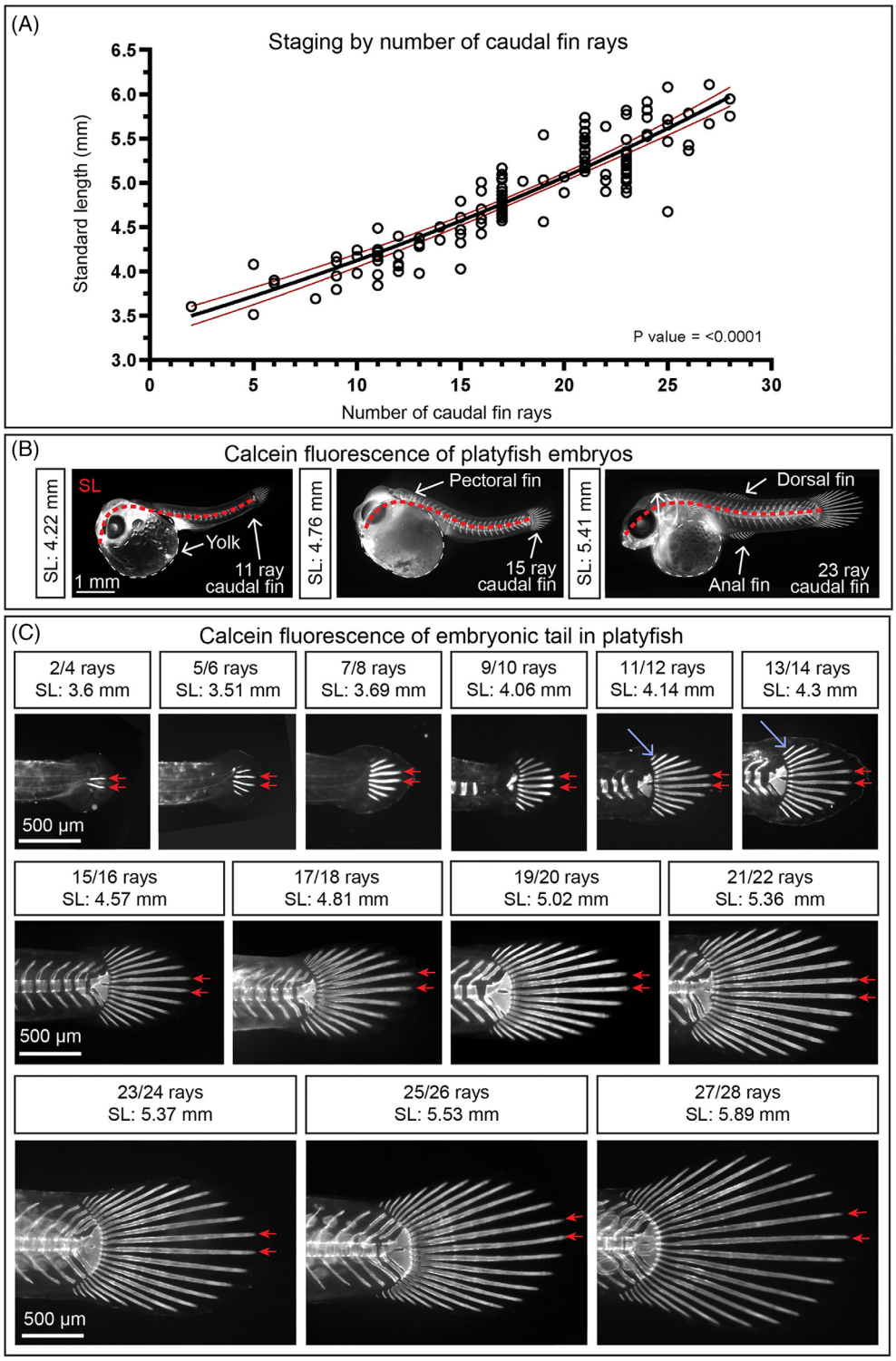

FIGURE 4 Development of the caudal skeleton in platyfish embryos dissected from euthanized gravid females (A) Extensive variation in growth rates of embryos developing internally in ovaries of gravid females. The standard length (from snout to caudal peduncle along the curvature of body axis) was plotted against the number of the caudal rays (x-axis). The curved black line depicts the nonlinear regression of the dataset, the brown lines depict the 95% confidence interval. R^2 value of 0.8275; $k = [0.01885–0.02228]$; P-value < 0.0001; $N = 128$ embryos (circles). (B) Images of representative embryos at different stages incubated with calcein, which strongly accumulates in osteoblasts. The red dashed line outlines standard length (SL). (C) Images of caudal fins at subsequent developmental stages of fin morphogenesis. Fin lepidotrichia (rays) are directly formed by dermal osteoblasts (without cartilaginous intermediates), and thus, they incorporate calcein during ray formation. The endoskeleton is initially cartilaginous and becomes replaced by ossified tissues during advanced development. The pair of medial rays is indicated with red arrows. The first ray above the hypural plate (purple arrows) is detected at 11/12-rays stage. SL, standard length in mm.

the middle rays. Importantly, at least one ray was clearly located above the hypural edge at the 11/12 ray stage, suggesting a contribution from the epichordal tissue. At the 13/14-ray stage, 2 rays were positioned dorsally to the hypural plate (Figure 4C). We concluded that the tissue above the notochord starts to participate in the caudal fin formation after the stage with 10 rays.

2.5 | Developmental dynamics of hypural plate formation

To further investigate the developmental relation between the endoskeleton and exoskeleton, we performed histological analysis using Alcian blue staining for cartilage and Alizarin red for calcified bones. At early

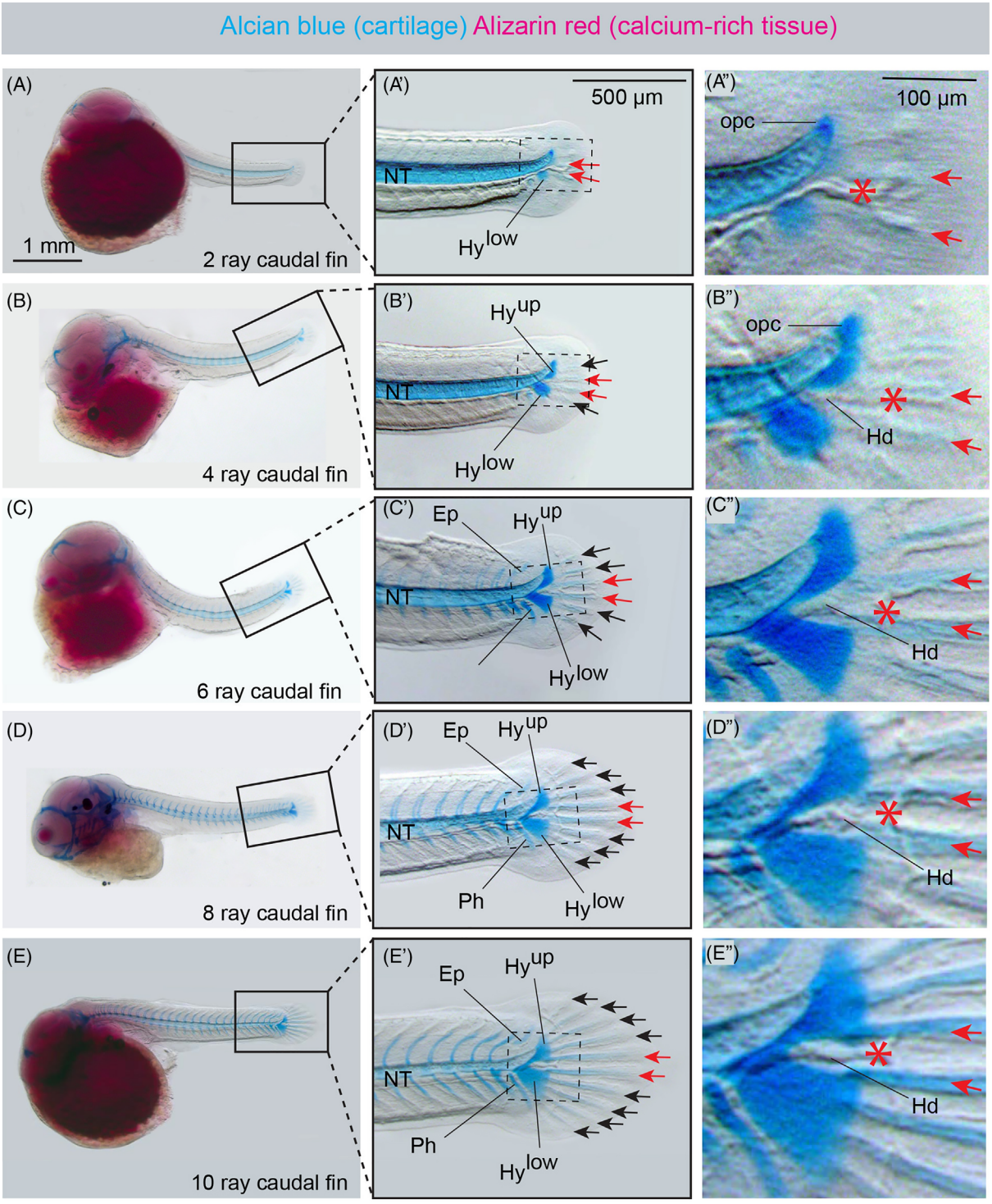

FIGURE 5 The upper and lower hypurals develop during the formation of the 10 principal caudal rays (A-E) Whole platyfish embryos stained with Alcian blue and Alizarin red to label cartilage and bone, respectively, at subsequent developmental stages defined by the number of caudal rays from 2 to 10. At this development time-window no ossification of the skeleton is observed by Alizarin red staining. The labeling of the yolk (a dark spheric structure on the image) with Alizarin red might indicate the presence of calcium in this tissue. The framed box on each image encircles the embryonic tail, which is magnified in the images with a primed corresponding letter. (A'-E') A higher magnification of the embryonic tail. The dashed-line frame depicts the tissue shown in a magnified view to the right. The earliest-forming pair of principal rays (red arrows) originate symmetrically around the hypural diastema (Hd) complex. New rays are added sequentially and symmetrically towards the upper and lower margin of the fin. (A"-E") The magnified images focused on the development of the lower and upper hypural plates, which start to be ankylosed at their base. The dorsoventral branching of the caudal vasculature (red asterisk) is situated in the hypural diastema, in the notch between the upper and lower hypural plates. NT, notochord; Ep, epural; Hy, hypural plate; Hd, hypural diastema; Ph, parahypural; opc, opisthural cartilage. $N = 7$ (number of specimens).

stages up to 9/10 rays, the lepidotrichia were unstained and visible mostly by contrast imaging, whereas the notochord and the vertebral elements displayed cartilaginous staining (Figure 5).

As in other teleosts, the earliest-forming pair of rays was detected at the site of the hypural diastema complex, which participates in the establishment of dorsoventral caudal fin symmetry in adult fish.[4] Indeed, the pioneering rays were formed by the connective tissue situated distally to the dorsal-ventral branching of the caudal vasculature, in the space between the lower (anterior) hypural plate (Hy^{low}) and the upper (posterior) hypural plate (Hy^{up}), which are compound elements in *Cyprinodontiformes* (Figure 5A).[6,57] The latter hypural plate was smaller and only weakly visible at the 2-ray stage (Figure 5A), but it became strongly stained at the 4-ray stage (Figure 5B). At the 6- and 8-ray stage, all lepidotrichia were positioned distally to the hypural plates (Figure 5C, D). At the 10-ray stage, the upper-most ray was aligned with the upper edge of the hypural plate at the tip of the notochord (Figure 5E). Thus, until this time point, the caudal fin attached normally to the hypochordal tissue.

The analysis of the Alcian blue stained embryos revealed another interesting observation. At 2-ray stage, the terminus of the notochord was covered by intensively labeled cap, which may correspond to the opisthural cartilage (opc) (Figure 5A"). At the next developmental stage, this notochord-associated cartilage became linked to the upper hypural plate (Figure 5B"). Indeed, at subsequent developmental stages, the dorsal edge of the upper hypural plate encompassed the tip of the notochord, suggesting an unusual epichordal extension of this compound structure (Figure 5C", D", E"). We concluded that the opisthural cartilage fused with the hypural element during fin formation, which would be a new finding that has never been reported in any other species. This anatomical peculiarity might correlate with losing the positional boundary, which normally limits the lobe with principal rays to the hypochordal part.

The process of matrix calcification became visible by Alizarin red staining in more advanced embryonic stages (Figure 6). At the 18-ray stage, which corresponds to the typical number of principal rays in the adult fin, 4 rays articulated with the dorsal processes (Figure 6A). Subsequent fin development was associated with symmetrical addition of upper rays attached to the epichordal tissues and lower rays attached to the hypochordal tissues (Figure 6B, C). We concluded that new upper rays of the platyfish caudal fin are attached to the tissue above the notochord after the 10-ray stage.

2.6 | Dorso-ventral symmetry of the adult caudal endoskeleton

To understand how the caudal endoskeleton was specialized in platyfish, we compared the morphology of the corresponding bones with three other fish species: zebrafish, medaka and guppies. We started from the posterior end, where the terminal compound vertebra provides the base for the dorsal uroneurals and ventral hypurals. While the zebrafish uroneural is a slender bone (Figure 2A′, E), the medaka, as previously shown,[58] lacks this element (Figure 2B′, F). Similarly, guppies also did not have this bone in the skeleton (Figure 2C′, G). In platyfish, we could detect only a vestigial outgrowth that corresponds to the rudimentary uroneural, also called stegural, consistent with our observations in embryos (Figure 2D′, H). We concluded that the uroneural is not developed in the two analyzed species of *Poeciliidae* family.

Hypurals are flattened bones that form ventrally to the notochord, but become the most-posterior bones at the tip of the dorsally-flexed notochord. While zebrafish had five separate hypurals (Figure 2A′, E) and medaka had two hypural plates (Figure 2B′, F), the platyfish and guppy tails displayed only one hypural plate with a fan-like shape (Figure 2C′, D′, G, H). Our developmental analysis of platyfish indicated that this single plate originates from two initially independent hypural plates that started fusing anteriorly along the notochord at the 8-ray stage (Figure 5D). In adult platyfish, a foramen (an elongated oval gap) was present in the base of the hypural plate, corresponding to the remnant of the hypural diastema during embryonic development (Figures 5 and 6). Microcomputed tomography revealed that the hypural plate was fused with the terminal compound vertebra (Figure 7). Thus, the extensive fusion of the hypurals into one plate, which is ankylosed with the terminal vertebra, represents a remarkable feature of the platyfish.

The preural-1, which is the anterior part of the terminal compound centrum, is typically associated with the epural, a dorsal/epichordal bone, and the parhypural, a ventral/hypochordal bone. In zebrafish and medaka, the epural had a slender rod-like structure, whereas in platyfish and guppies, this bone had a flattened form (Figure 2). As opposed to zebrafish and medaka, in platyfish and guppies, the epural mirrored the shape of the ventrally located counterpart, the parhypural. In both *Poeciliidae* species, in the neural (dorsal) and haemal (ventral) spines of the preural-2 vertebra displayed a distally widened shape and carried blade-like plates with a mirrored appearance, which contrasts thin spines in zebrafish and medaka. Thus, in platyfish and guppies, the

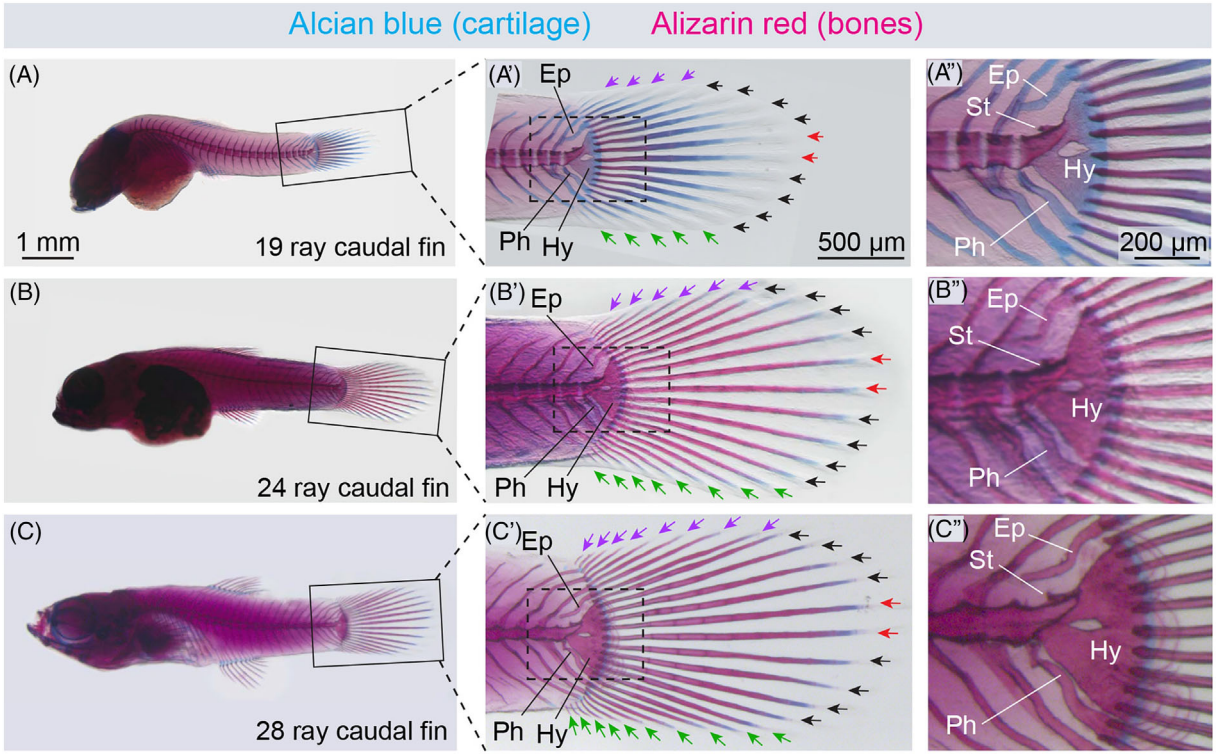

FIGURE 6 Calcification of the endoskeleton coincides with the fusion of the upper and lower hypural at the posterior margin (A-C) Whole embryos stained with Alcian blue and Alizarin red to label cartilage and bone, respectively, at advanced developmental stages. The yolk is markedly decreased, consistent with the growth of the embryos. The framed box on each image encompasses the embryonic tail, which is magnified in the images with a primed corresponding letter. (A'-C') Higher magnifications of the embryonic tail. The dashed-line frame depicts the tissue shown in a magnified view to the right with the same letter and a double prime symbol. The medial rays are indicated with red arrows. The lateral principal rays that articulate with hypurals are pointed with black arrows. The upper rays that articulate with the epichordal (dorsal) tissue are highlighted with purple arrows. The lower rays that articulate with the hypochordal (ventral) tissue are depicted with green arrows. (A") The ossification of the endoskeleton is associated with the fusion of the hypurals at their posterior-most margin. An oval gap is remaining in the middle of the plate. (B″ and C″) An elongated hole in the hypural plate persists throughout the embryonic development. Ep, epural; Hy, hypural; Ph, parahypural; St, stegural (vestigial uroneural). $N = 28$ (number of specimens).

caudal skeleton displayed a higher level of dorsoventral symmetry.

Interestingly, we identified a difference between both *Poeciliidae* species in blade-like plates, which widen the base of the mentioned bones. These blade-like plates had a serrated edge in guppies (Figure 2C′, G), whereas a straight margin in platyfish (Figure 2D′, H). Furthermore, in guppies, the pattern of notches in these bony ridges was not identical on the dorsal and ventral counterparts. This variation in detailed serration led to a decreased dorsoventral symmetry of the skeleton in guppies, compared to platyfish. Nevertheless, both poeciliids displayed overall similar morphological modification of the epi- and hypochordal spines, reinforcing the internal dorsoventral symmetry of their caudal endoskeleton.

Beside symmetry-boosting modifications of the dorsal spines in platyfish, we found that the number of vertebrae with supportive bones for the caudal fin was higher in platyfish and guppies than in the zebrafish and medaka. In the two latter species, the terminal compound centrum (CC) and two preurals (PU-2 and PU-3) participated in the support of the caudal rays, as reported[43,46] (Figure 2A′, B′, E, F). In both poeciliids, beside these 3 vertebrae, another anterior preural 4 (PU-4) contributed to radials of the caudal fins. In 25% of examined platyfish specimens, neural spines of preural 5 (PU-5) articulated with the procurrent upper rays (3 out of 12 specimens) (Figure 2D′, H). Thus, the platyfish and guppy caudal fins were supported by the endoskeleton involving the terminal compound centrum and four to occasionally five separate preurals, offering a greater number of supports compared to zebrafish and medaka.

3 | DISCUSSION

The caudal fin of the teleost has evolved an external dorsoventral symmetry, characterized by a nearly mirrored distribution of principal rays in the upper and lower

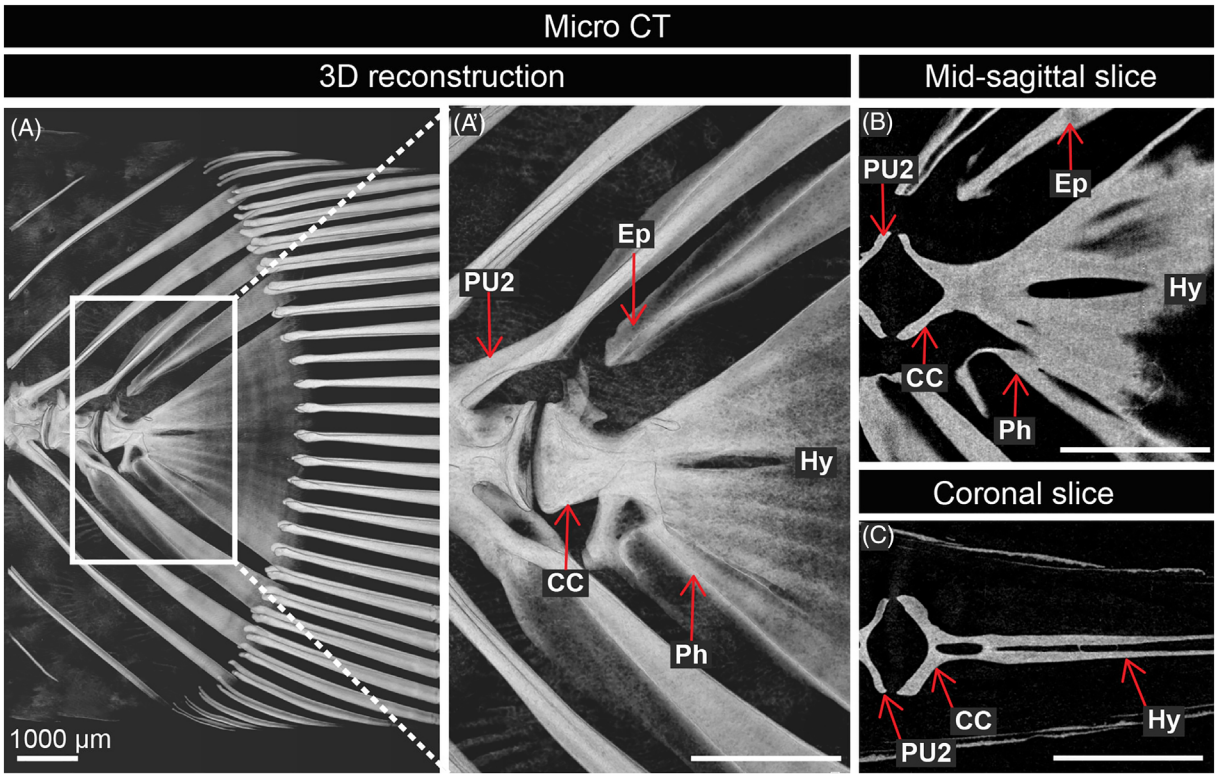

FIGURE 7 Micro-computed tomography (µCT) reconstructions of the caudal skeleton of adult platyfish (A) 3D-reconstructed µCT of the adult caudal endoskeleton to visualize bones. (A') A magnified area of the frame shown in (A). Note the fusion of the terminal compound centrum (CC) and the hypural plate (Hy). (B, C) Mid-sagittal and coronal 2D slices display the continuity of the terminal compound centrum and the hypural plate, indicating complete ankylosis of these bones. Ep, epural; Hy, hypural; Ph, parahypural; CC, terminal compound centrum PU2, preural 2.

lobes. This trait, however, is not reflected by the associated endoskeleton that retained its ancestrally derived ventral identity. Here, we provide evidence that the bauplan of the teleost fin is exceptionally innovative in two *Poeciliidae* species, the platyfish and the guppy, which bypassed the constraint of the ventral attachment of principal rays and achieved a high degree of internal symmetry.

Our main finding is that 3–4 dorsal principal rays articulate with the epural and neural spine, which are bones of epichordal origin. This contribution of the dorsally derived elements to the principal field of the caudal fin represents an atypical pattern in extinct and living teleosts, according to the broadly accepted conventions formulated by Schultze and Arratia.[6,7] The epichordal identity of the 3–4 principal rays might be a distinctive trait for the *Poeciliidae* family. A recently described new species of *Cyprinodontiformes*, named *Pseudorestias lirimensis*, forms an articulation between the first principal ray and epural.[59] Interestingly, the *Cyprinodontiform* fossil from the oligocene in France, †*Prolebias delphinensis*, reveals a configuration, in which the upper non-branched principal ray articulated with the neural spine.[60,61] In this extinct species, the caudal fin consisted of 12 branched rays, whereby the upper-most branched ray connected to the epural. Thus, the involvement of epichordal tissue to the bauplan of the caudal skeleton might be common to the poeciliids and potentially to other families of the *Cyprinodontiform* order.

3.1 | Hypothetical morphogenetic boundaries and organizers of the caudal fin

We do not yet know how poeciliids could bypass the constraint of the caudal fin ventral identity that is outlined by the notochord position. Developmental analysis can provide valuable cues about homologies emerging during ontogenesis.[4] Studies of some teleosts have led to a hypothesis that a boundary landmark for the upper limit of principal rays corresponds to the opisthural cartilage, which is formed by the posterior tip of the notochord.[8,57,62] In medaka, the opisthural cartilage has been reported to become ossified and fused to ural centrum 2 during fin development.[58] In adult zebrafish, the opisthural cartilage remains non-ossified at the ventral

edge the procurrent ray, above the first principal ray[4,53] (Figure 2A′, E). We observed that in platyfish embryos, the opisthural cartilage fused with the hypural element during early fin formation (Figure 5A"–C"), which might be a unique characteristic among teleosts. This finding suggests that the anatomical landmark for the presumptive boundary between the upper principal and procurrent rays becomes reduced already at the onset of fin development. It is tempting to hypothesize that the joining of notochord-associated boundary with a hypural element would permit or facilitate an evolutionary path for the formation of principal rays in the epichordal part of the body.

Developmental principles regulating external symmetry of the caudal fin, which is characterized by equal dorsal and ventral halves, have been recently addressed using transgenic reporters in zebrafish.[63] In that study, monitoring of ray emergence indicates an interplay between three morphogenetic fields, namely a central organizer at the hypural diastema and two peripheral organizers at the upper and lower margins of the caudal fin.[63] Platyfish appear to adhere to the model of a central organizer, since our histological analysis show that rays are sequentially added from the hypural diastema outwards (Figures 5 and 6). In contrast, our data with calcein staining of platyfish embryos did not reveal any early separate emergence of bounding principal rays (Figure 4C). This suggests that in platyfish, the hypothetical peripheral organizers might be synchronized with the morphogenetic activity of the central organizer. Further research is warranted to elucidate the position of ray organizers relative to the caudal endoskeleton in platyfish.

3.2 | *zic1/4* genes are markers of epichordal rays in the platyfish caudal fin

The exoskeletal fin rays differentiate together with the endoskeletal radials, the patterning of which occurs along the anterior-posterior axis during development.[64] Cell lineage tracing analysis in medaka demonstrated that bones and their attached rays develop from the same population of mesoderm-derived mesenchyme.[13] In this study, we inferred the dorso-ventral identity of rays from their connection to the endoskeleton. Our developmental analysis of platyfish revealed that the first dorsally attached ray is formed starting at the 10-ray stage of the caudal fin. Given that 10 central rays are attached to the hypural plate, our interpretation of this finding is that dorsal and ventral rays become symmetrically distributed on each side during their formation.

The molecular basis of the mechanisms increasing the contribution of epichordal tissue in the caudal skeleton might involve the regulation of *zic1* and *zic4* expression. These zinc-finger transcription factors were highly expressed in the three uppermost principal rays as compared to the other rays, as shown by qRT-PCR. Studies in medaka demonstrated that *zic1* and *zic4* are epichordal marker genes.[47] A mutation of the *zic1/4* enhancer, called *Double anal fin* (*Da*), causes a ventralized phenotype of the body, in which caudal fin rays articulate with both hypurals and epurals.[48,54] In another species, called Siamese fighting fish (*Betta splendens*; order *Perciformes*), a double-tail mutant has been associated with a deletion of a *zic1/4* enhancer.[65] Both in medaka and Siamese fighting fish, *zic1* and *zic4* were suppressed in double tail mutants, suggesting a conserved mechanism for dorsal duplication of the caudal fin lobe in teleosts. In platyfish, we found that *zic1* and *zic4* were expressed in the three upper principal rays, providing molecular evidence of the epichordal origin of these structures. How these master genes regulate the innovative bauplan of the platyfish tail requires further studies.

3.3 | Advancements of the caudal endoskeletal bauplan in *Cyprinodontiformes*

The next striking feature of the caudal skeleton in platyfish and guppies is a high degree of dorsoventral symmetry of the supporting bones. This observation is consistent with the main feature of *Cyprinodontiformes*, which evolved enhanced symmetry of its caudal endoskeleton, as reported for various species.[58-60,66-69] In this order, the upper and lower hypural plates can stay separate or fuse to provide a more rigid support for the principal rays. Consistently, our developmental analysis of platyfish demonstrated that the hypural plate derives from two separate elements, namely a lower hypural plate (ie, hypurals 1 + 2 in zebrafish) and an upper hypural plate (ie, hypurals 3 + 4 + 5). They become ankylosed to form a single bone, starting at the 18-ray stage of the caudal fin, leading to the disappearance of hypural diastema. An anterior gap in this plate remains visible in platyfish, as in most poeciliids,[58,60] and may permit the passage of caudal vasculature. Importantly, a symmetrical fan-like hypural plate provides a support for equidistant rays at the center of the fin. This regularly spaced sequence of rays contrasts with the typical situation of other teleosts, including zebrafish and medaka, in which a wider interspace between the lower and upper hypural groups is demarcated by a hiatus between the corresponding rays.[70] Thus, as compared to the bauplan with separated

hypural elements, one hypural plate uniformly consolidates the structural support for the fin and it enhances the regularity of ray distribution.

The *Cyprinodontiformes* can be unambiguously recognized by the presence of a single, blade-like epural that mirrors the parhypural, and the widened neural and hemal spines.[58-60,66-69] Consistently, the next level of the caudal endoskeletal symmetry in platyfish and guppies is represented by these structures. In both these species, the dorsal and ventral counterpart bones of preural centra display mirrored appearance and they symmetrically support upper and lower principal rays. Indeed, the shape of epural and parhypural bones of the terminal vertebra, as well as the neural and haemal spines of preural-2, were similarly flattened with a wider distal end, and with protruding blade-like ridges. In platyfish, these thin ridges had straight margins, whereas in the analyzed guppy species (*Poecilia reticulata*), they were serrated. Interestingly, a study of another guppy species, *Poecilia mexicana*, has shown that the counterpart bones bear straight edges, suggesting the existence of endoskeleton variations among the same genus.[71] This observation supports a hypothesis about powerful evolvability within this taxonomic group.

From the functional perspective, the stunning internal symmetry of the platyfish and guppy caudal skeleton might further advance the hydrodynamic characteristics of the tail.[10,72] This could be of advantage as compared to an internally asymmetrical bauplan of the typical homocercal fin. The biophysical properties could be compared between distinct types of caudal fins with a different degree of the endoskeletal symmetry. An interesting question is to determine how the evolutionarily innovative architecture of the poeciliid caudal fin translates to the swimming performance.

4 | EXPERIMENTAL PROCEDURES

4.1 | Fish strains and animal procedures

The following fish were used for this study: zebrafish (*Danio rerio*) AB strain (Oregon) at approximately 3 cm standard length, platyfish (*Xiphophorus maculatus*) strain Bleeding Heart, Mickey Mouse or Gold platy at approx. 3.3 cm standard length, guppies (*Poecilia reticulata*) at approximately 3 cm standard length, medaka (*Oryzias woworae*) of approximately 2 cm standard length. The standard length was measured from the snout to the caudal peduncle, without including the caudal fin. Adult platyfish, guppies and medaka were purchased from a commercial aquarium fish vendor (Aqualand, Renens/Lausanne, Switzerland). Zebrafish were bred in our fish facility.

Animal euthanasia was performed by immersion in 300 mg/L tricaine solution (MS-222; Sigma-Aldrich) for approx. 10 minutes. Then, the hearts were dissected from the euthanized fish. This procedure was performed in accordance with Swiss regulations and was approved by the Cantonal Veterinary office of Fribourg, Switzerland.

Adult tails were cut with a sharp razor blade from euthanized fish after heart removal. Platyfish embryos were dissected from similarly euthanized gravid females using a pair of sterilized dissection scissors. The entire ovary was placed in system water and embryos were removed from follicles and manually dechorionated with tweezers.

4.2 | Histological staining

A two-color acid free staining technique with Alcian blue and Alizarin red solution was used as described previously.[73] Two stock staining solutions were prepared as Part A and Part B and stored at room temperature. The Part A component contained 0.02% Alcian blue dissolved in 70% Ethanol with 60 mM $MgCl_2$. Preparation of this solution required two steps. Firstly, 0.4 *g* Alcian blue 8GX (Sigma-Aldrich, A5268) was dissolved in 50 ml of 50% ethanol at 37°C on a shaker. After the powder has dissolved, 50 ml of 90% ethanol was added and mixed. In the last step, 5 ml of this solution was combined with 70 ml of 95% ethanol, 6 ml of 1 M $MgCl_2$ and 19 ml water. The Part B consisted of 5% Alizarin red S (Sigma-Aldrich, A5533) dissolved in distilled water. The final double staining solution was prepared freshly before staining by mixing 10 ml of Part A with 200 µl of Part B.

The fins of adult fish were fixed in a petri dish in 4% paraformaldehyde in PBS for 2 days at room temperature. Embryos were fixed overnight at room temperature. Specimens were then rinsed and washed with PBS twice for 20–30 minutes each. For dehydration prior to staining, adult specimens underwent an ethanol series as follows: 70% - 80% - 90% - 100% for 1 hour each. For embryos, a 15-minute dehydration step in 50% ethanol sufficed. Fins and embryos were rocked overnight at room temperature in the Part A/Part B double staining solution, followed by rinsing in distilled water to remove excess dye. Specimens were subsequently bleached to remove pigmentation, using a 1:1 ratio of 2% potassium hydroxide and 3% hydrogen peroxide during 1–3 hours for adults and 20–30 minutes for embryos.

In order to clear the specimens to visualize the bones, adult fins were incubated in an enzyme solution of borax (3:7 saturated borax solution to distilled water) and

trypsin (0.1%; Sigma-Aldrich, T4799) during 3 days. Scales also stain lightly with the double stain solution, so these were removed in distilled water using forceps. For imaging and storage, fins and embryos were transferred to glycerol using a graded series of 0.5% potassium hydroxide and glycerol solutions (3:1, 1:1, 1:3; for at least 2 hours or overnight) and finally stored in 100% glycerol and imaged.

Color images were taken with a Leica AF M205 FA stereomicroscope equipped with a digital camera (Leica Microsystems, Wetzlar, Germany).

4.3 | Calcein labeling of embryos and developmental staging

0.2% calcein (Sigma-Aldrich, C0875) solution was prepared in system water. Due to calcein's strong acidifying affects, we adjusted the pH to 7.2 by adding an appropriate amount of 1 *N* sodium hydroxide. Live platyfish embryos were immersed in this solution for 15 minutes in petri dishes, rinsed several times in system water during approx. 30 minutes. The embryos were then euthanized in 300 mg/L tricaine solution. Fluorescent images of embryos were taken with a Leica AF M205 FA stereomicroscope using a GFP2 filter (Leica Microsystems, Wetzlar, Germany).

The standard length was measured from the snout to the caudal peduncle, not including the caudal fin and following the body axis, using ImageJ (NIH, Bethesda, Maryland, United-States). Developmental staging was based on caudal fin morphogenesis, which was assessed by counting caudal rays. These two parameters were plotted together using Prism (Graphpad, San Diego, California), where a nonlinear regression curve was calculated.

4.4 | Quantitative real-time polymerase chain reaction analysis

Ray triplets were excised from caudal fins with a scalpel: uppermost principal rays 1, 2 and 3 (upR 1–3), upper principal rays 6, 7 and 8, counted from the top (upR 6–8) and lower principal rays 1, 2 and 3, counted from the bottom (loR 1–3). Tissues from three fish were collected and pooled together per one sample. Each sample was reproduced in triplicates, deriving from other groups of three fish. Collected fin tissues were frozen immediately on dry ice and homogenized in Qiazol Lysis Reagent (Qiagen, Hilden, Germany) using a Polytron tissue homogenizer. RNA was extracted using chloroform and isolated from tissue debris using MaXtract high density columns (Qiagen, Hilden, Germany). RNA was precipitated using isopropanol and resuspended in water. cDNA was synthetized using the Superscript IV reverse transcriptase (Thermo Fishers, Waltham, Massachusetts, United-States), following the manufacturer's protocol. qRT-PCR was performed using the Kapa SYBR Fast qPCR kit (Kapa Biosystems, Wilmington, Massachusetts, United-States) following the manufacturer's guidelines. The following primers were used:

actb2 (XM_005806049.2): Fw: 5′-CGTGCGGGATATCATTTGCCTG-3′; Rev: 5′-ACAACCAGTGCGGCGATTTC-3′.

pabp (XM_005797394.2): Fw: 5′-CCAGAGTCTCTCCGCTCCAAG-3′; Rev: 5′-TGGGACAACGGCTGAGTTGG-3′.

zic1 (XM_005797813.2): Fw: 5′-CACGTCGGACAAGCCGTATC-3′; Rev: 5′- GCAGGGTTGGTGGATTCGTG-3′.

zic4 (XM_005797812.2): Fw: 5′-GCGGTAAAGTGTTTGCAAGATCC-3′; Rev: 5′-TGTCGCTACTGTTGGCGAAG-3′.

Normalized gene expression was calculated using the delta CT method. Gene expression levels were averaged over 3 cDNAs per ray type and two technical replicates. Results were plotted in Graphpad Prism (Graphpad, San Diego, California, United-States).

4.5 | Micro computed tomography

The tails collected from euthanized fish were fixed in 4% paraformaldehyde in a petri dish for 2 days at room temperature. The specimens were then dehydrated in 70% ethanol for one hour and transferred into a transparent plastic tube with 70% ethanol.

Micro CT images with a voxel size of 3 μm were acquired using a Bruker SkyScan 2211 X-ray microscopy platform, equipped with an 11-megapixel CCD panel. Image reconstruction was performed using NRecon software (Bruker Corporation, Germany) and Avizo (Thermo Fisher Scientific).

4.6 | Terminology

The terminology follows the conventions formulated by Schultze and Arratia.[6,7,12]

Centrum or vertebral centrum: A mineralized, ossified, or partly cartilaginous/ossified element that surrounds the notochord.

Compound centrum (CC): terminal vertebral centrum at the posterior region of the caudal endoskeleton comprising preural centrum 1 and ural centra.

Epural: Detached neural spine of a terminal compound vertebra that commonly supports one or more dorsal procurrent rays.

Hypural: Modified haemal spine (of an ural centrum) that has lost its haemal arch and canal.

Hypural diastema: Space positioned between the lower and upper hypural plates.

Opisthural cartilage (opc): Cartilage at the posterior extremity of the notochord. It can extend distally between the uppermost (unbranched) principal ray and the procurrent fin ray above it. It is considered to define the upper limits of the field with principal caudal rays.

Opisthural gap: A space between the upper bounding principal ray and the adjacent procurrent ray. This gap corresponds to the upper limit of the caudal principal ray field.

Parhypural: The parhypural is the haemal spine of preural centrum 1, which is fused within terminal compound vertebra.

Preural centrum: Vertebral centrum of the caudal region preceding the ural centra, bearing both neural and haemal arches and usually both neural and haemal spines, each of which supports a caudal ray at its distal tip. Preural centra are numbered from the posterior-most to the anterior-most.

Procurrent caudal ray: Procurrent rays are short rays, shorter than the principal ones, which form the anterior series of lepidotrichia of median fins and which are associated with endoskeletal elements.

Principal caudal rays: Principal rays of the caudal fin are all the segmented and branched rays plus normally one unbranched but segmented ray located at the leading margin in each lobe of the fin.

Stegural: Modified anterior-most uroneural bearing membranous bony extension at its antero-dorsal border.

Uroneurals: Modified neural arches that extend from the ural centrum dorsally to the notochord.

AUTHOR CONTRIBUTIONS

Lana Rees: Investigation (equal); methodology (equal); project administration (equal); writing – review and editing (equal). **Désirée König:** Conceptualization (supporting); data curation (supporting); investigation (supporting); methodology (equal); writing – review and editing (equal). **Anna Jazwinska:** Conceptualization (lead); funding acquisition (lead); investigation (equal); methodology (equal); resources (lead); supervision (lead); validation (equal); writing – original draft (lead); writing – review and editing (equal).

ACKNOWLEDGMENTS

The authors thank Verena Zimmermann for zebrafish facility management and husbandry. Special acknowledgments are dedicated to Dr. Christoph Neururer from the Computer X-Ray Tomography Facility, Department of Geoscience, University of Fribourg. We thank Tim Meili for designing the schematic drawing of the caudal skeleton during his bachelor work in our lab. We appreciate the agreement of Dr. Gloria Arratia (University of Kansas) to include her drawing in our introductory figure. We thank Dr. C. Pfefferli for critical reading of the manuscript and the members of the Jaźwińska lab for input on the study. Open access funding provided by Universite de Fribourg.

FUNDING INFORMATION

This research was funded by the Swiss National Science Foundation and the University of Fribourg.

CONFLICT OF INTEREST

The authors declare no conflict of interest.

DATA AVAILABILITY STATEMENT

All raw data and imaging files are available upon request from the authors.

ORCID

Anna Jaźwińska https://orcid.org/0000-0003-3881-9284

REFERENCES

1. Flammang BE. The fish tail as a derivation from axial musculoskeletal anatomy: an integrative analysis of functional morphology. *Fortschr Zool*. 2014;117(1):86-92. doi:10.1016/j.zool.2013.10.001
2. Metscher B, Ahlberg P. Origin of the teleost tail: phylogenetic frameworks for developmental studies. In: Ahlberg PE, ed. *Major Events in Early Vertebrate Evolution: Palaeontology, Phylogeny, Genetics, and Development*. New York: Taylor & Francis; 2001:333-349.
3. Sallan L. Fish 'tails' result from outgrowth and reduction of two separate ancestral tails. *Curr Biol*. 2016;26(23):R1224-R1225. doi:10.1016/j.cub.2016.10.036
4. Desvignes T, Carey A, Postlethwait JH. Evolution of caudal fin ray development and caudal fin hypural diastema complex in spotted gar, teleosts, and other neopterygian fishes. *Dev. Dyn*. 2018;247(6):832-853. doi:10.1002/dvdy.24630
5. Goodrich ES. *Studies on the Structure and Development of Vertebrates*. London: Macmillen; 1930.
6. Schultze H-P, Arratia G. The caudal skeleton of basal teleosts, its conventions, and some of its major evolutionary novelties in a temporal dimension. In: Arratia G, Schultze H-P, Wilson MVH, eds. *Mesozoic Fishes 5—Global Diversity and Evolution*. München: Verlag Dr. Friedrich Pfeil; 2013:187-246.
7. Arratia G. Complexities of early Teleostei and the evolution of particular morphological structures through time. *Copeia*. 2015;103(4):999-1025. doi:10.1643/cg-14-184
8. Schultze H-P, Arratia G. The composition of the caudal skeleton of teleosts (Actinopterygil: Osteichthyes). *Zool J Linn Soc*. 1989;97(3):189-231. doi:10.1111/j.1096-3642.1989.tb00547.x
9. Lauder GV. Function of the caudal fin during locomotion in fishes: kinematics, flow visualization, and evolutionary patterns. *Am Zool*. 2000;40(1):101-122. doi:10.1093/icb/40.1.101

10. Lauder GV. Flexible fins and fin rays as key transformations in ray-finned fishes. In: Dial KP, Shubin N, Brainerd EL, eds. *Great Transformations in Vertebrate Evolution*. Chicago: University of Chicago Press; 2015:31-45.
11. Hadzhiev Y, Lele Z, Schindler S, et al. Hedgehog signaling patterns the outgrowth of unpaired skeletal appendages in zebrafish. *BMC Dev Biol*. 2007;7(1):75. doi:10.1186/1471-213X-7-75
12. Arratia G. Actinopterygian postcranial skeleton with special reference to the diversity of fin ray elements, and the problem of identifying homologies. In: Arratia G, Schultze H-P, Wilson MVH, eds. *Mesozoic Fishes 4—Homology and Phylogeny*. München: Verlag Dr. Friedrich Pfeil; 2008:49-101.
13. Shimada A, Kawanishi T, Kaneko T, et al. Trunk exoskeleton in teleosts is mesodermal in origin. *Nat Commun*. 2013;4:1639. doi:10.1038/ncomms2643
14. Nelson J, Grande T, Wilson M. *Fishes of the World*. 5th ed. Hoboken, New Jersey: Wiley; 2016:1-707.
15. Betancur-R R, Wiley EO, Arratia G, et al. Phylogenetic classification of bony fishes. *BMC Evol Biol*. 2017;17(1):162. doi:10.1186/s12862-017-0958-3
16. Evans J, Pilastro A, Schlupp I. *Ecology and Evolution of Poeciliid Fish*. Chicago: The University of Chicago Press; 2011.
17. Rosen DE, Bailey RM. The poeciliid fishes (Cyprinodontiformes), their structure, zoogeography and systematics. *Bull Am Mus Nat Hist*. 1963;126:1-176.
18. Tavolga WN. Embryonic development of the platyfish (Platypoecilus), the swordtail (*Xiphophorus*), and their hybrids. *Bulletin of the AMNH*. 1949;94: Article 4:165-229 .
19. Bailey RT. The ovarian cycle in the viviparous teleost *Xiphophorus* Helleri. *Biol Bull*. 1933;64(2):206-225.
20. Pollux BJA, Pires MN, Banet AI, Reznick DN. Evolution of placentas in the fish family Poeciliidae: an empirical study of macroevolution. *Annu Rev Ecol Evol Syst*. 2009;40(1):271-289. doi:10.1146/annurev.ecolsys.110308.120209
21. Jones JC, Fruciano C, Keller A, Schartl M, Meyer A. Evolution of the elaborate male intromittent organ of *Xiphophorus* fishes. *Ecol Evol*. 2016;6(20):7207-7220. doi:10.1002/ece3.2396
22. Schartl M, Kneitz S, Ormanns J, et al. The developmental and genetic architecture of the sexually selected male ornament of swordtails. *Curr Biol*. 2021;31(5):911-922.e4. doi:10.1016/j.cub.2020.11.028
23. Bischoff RJ, Gould JL, Rubenstein DI. Tail size and female choice in the guppy (Poecilia reticulata). *Behav Ecol Sociobiol*. 1985;17(3):253-255. doi:10.1007/BF00300143
24. Tobler M, Kelley JL, Plath M, Riesch R. Extreme environments and the origins of biodiversity: adaptation and speciation in sulphide spring fishes. *Mol Ecol*. 2018;27(4):843-859. doi:10.1111/mec.14497
25. Essenberg TM. Complete sex-reversal in the viviparous teleost *Xiphophorus helleri*. *Biol Bull*. 1926;51(2):98-111.
26. Schartl M. Beyond the zebrafish: diverse fish species for modeling human disease. *Dis Model Mech*. 2013;7:181-192. doi:10.1242/dmm.012245
27. Schartl M, Walter RB. *Xiphophorus* and Medaka cancer models. In: Langenau DM, ed. *Cancer and Zebrafish: Mechanisms, Techniques, and Models*. Cham: Springer International Publishing; 2016:531-552.
28. Kallman KD. The platyfish, *Xiphophorus maculatus*. In: JKing RC, ed. *Handbook of Genetics. Vertebrates of Genetic Interest*. Vol 4. New York: Plenum; 1975:81-132.
29. Patton EE, Mitchell DL, Nairn RS. Genetic and environmental melanoma models in fish. *Pigment Cell Melanoma Res*. 2010;23(3):314-337. doi:10.1111/j.1755-148X.2010.00693.x
30. Meierjohann S, Schartl M. From Mendelian to molecular genetics: the *Xiphophorus* melanoma model. *Trends Genet*. 2006;22(12):654-661. doi:10.1016/j.tig.2006.09.013
31. Walter R, Kazianis S. *Xiphophorus* interspecies hybrids as genetic models of induced neoplasia. *ILAR J*. 2001;42(4):299-321.
32. Kang JH, Schartl M, Walter RB, Meyer A. Comprehensive phylogenetic analysis of all species of swordtails and platies (Pisces: Genus *Xiphophorus*) uncovers a hybrid origin of a swordtail fish, *Xiphophorus* monticolus, and demonstrates that the sexually selected sword originated in the ancestral lineage of the genus, but was lost again secondarily. *BMC Evol Biol*. 2013;13:25. doi:10.1186/1471-2148-13-25
33. Basolo AL. Genetic linkage and color polymorphism in the southern Platyfish (*Xiphophorus* maculatus): a model system for studies of color pattern evolution. *Zebrafish*. 2006;3(1):65-83. doi:10.1089/zeb.2006.3.65
34. Amores A, Catchen J, Nanda I, et al. A RAD-tag genetic map for the platyfish (*Xiphophorus* maculatus) reveals mechanisms of karyotype evolution among teleost fish. *Genetics*. 2014;197(2):625-641. doi:10.1534/genetics.114.164293
35. Schartl M, Walter RB, Shen Y, et al. The genome of the platyfish, *Xiphophorus* maculatus, provides insights into evolutionary adaptation and several complex traits. *Nat Genet*. 2013;45(5):567-572. doi:10.1038/ng.2604
36. Braasch I, Peterson SM, Desvignes T, McCluskey BM, Batzel P, Postlethwait JH. A new model army: emerging fish models to study the genomics of vertebrate Evo-Devo. *J Exp Zool B Mol Dev Evol*. 2015;324(4):316-341. doi:10.1002/jez.b.22589
37. Takeda H, Shimada A. The art of Medaka genetics and genomics: what makes them so unique? *Annu Rev Genet*. 2010;44(1):217-241. doi:10.1146/annurev-genet-051710-151001
38. Kirchmaier S, Naruse K, Wittbrodt J, Loosli F. The genomic and genetic toolbox of the teleost medaka (Oryzias latipes). *Genetics*. 2015;199(4):905-918. doi:10.1534/genetics.114.173849
39. Betancur-R R, Broughton RE, Wiley EO, et al. The tree of life and a new classification of bony fishes. *PLoS Currents*. 2013;5. doi:10.1371/currents.tol.53ba26640df0ccaee75bb165c8c26288
40. Hughes LC, Ortí G, Huang Y, et al. Comprehensive phylogeny of ray-finned fishes (Actinopterygii) based on transcriptomic and genomic data. *PNAS*. 2018;115:6249-6254. doi:10.1073/pnas.1719358115
41. Santoriello C, Zon LI. Hooked! Modeling human disease in zebrafish. *J Clin Investig*. 2012;122(7):2337-2343. doi:10.1172/jci60434
42. Marques IJ, Lupi E, Mercader N. Model systems for regeneration: zebrafish. *Dev*. 2019;146(18). doi:10.1242/dev.167692
43. Bird NC, Mabee PM. Developmental morphology of the axial skeleton of the zebrafish, Danio rerio (Ostariophysi: Cyprinidae). *Dev Dyn*. 2003;228(3):337-357. doi:10.1002/dvdy.10387
44. Pfefferli C, Jaźwińska A. The art of fin regeneration in zebrafish. *Regeneration*. 2015;2(2):72-83. doi:10.1002/reg2.33
45. Sehring IM, Weidinger G. Recent advancements in understanding fin regeneration in zebrafish. *WIREs Dev Biol*. 2020;9(1):e367. doi:10.1002/wdev.367

46. Fujita K. Caudal skeleton ontogeny in the Adrianichthyid fish, Oryzias Latipes. *J Phytopathol*. 1992;39(1):107-109.
47. Ohtsuka M, Kikuchi N, Yokoi H, et al. Possible roles of zic1 and zic4, identified within the medaka double anal fin (Da) locus, in dorsoventral patterning of the trunk-tail region (related to phenotypes of the Da mutant). *Mech Dev*. 2004; 121(7):873-882. doi:10.1016/j.mod.2004.04.006
48. Moriyama Y, Kawanishi T, Nakamura R, et al. The Medaka zic1/zic4 mutant provides molecular insights into teleost caudal fin evolution. *Curr Biol*. 2012;22(7):601-607. doi:10.1016/j.cub.2012.01.063
49. König D, Jaźwińska A. Zebrafish fin regeneration involves transient serotonin synthesis. *Wound Repair Regen*. 2019;27: 375-385. doi:10.1112/wrr.12719
50. Wiley EO, Fuiten AM, Doosey MH, Lohman BK, Merkes C, Azuma M. The caudal skeleton of the zebrafish, Danio rerio, from a phylogenetic perspective: a Polyural interpretation of homologous structures. *Copeia*. 2015;103(4):740-750. doi:10.1643/CG-14-105
51. Bensimon-Brito A, Cancela ML, Huysseune A, Witten PE. The zebrafish (Danio rerio) caudal complex - a model to study vertebral body fusion. *J Appl Ichthyol*. 2010;26:235-238.
52. Bensimon-Brito A, Cancela ML, Huysseune A, Witten PE. Vestiges, rudiments and fusion events: the zebrafish caudal fin endoskeleton in an evo-devo perspective. *Evol Dev*. 2012;14(1): 116-127. doi:10.1111/j.1525-142X.2011.00526.x
53. Cumplido N, Allende ML, Arratia G. From Devo to Evo: patterning, fusion and evolution of the zebrafish terminal vertebra. *Front Zool*. 2020;17(1):18. doi:10.1186/s12983-020-00364-y
54. Kawanishi T, Kaneko T, Moriyama Y, et al. Modular development of the teleost trunk along the dorsoventral axis and zic1/zic4 as selector genes in the dorsal module. *Development*. 2013;140(7):1486-1496. doi:10.1242/dev.088567
55. Du SJ, Frenkel V, Kindschi G, Zohar Y. Visualizing normal and defective bone development in zebrafish embryos using the fluorescent chromophore calcein. *Dev Biol*. 2001;238(2):239-246. doi:10.1006/dbio.2001.0390
56. Parichy DM, Elizondo MR, Mills MG, Gordon TN, Engeszer RE. Normal table of postembryonic zebrafish development: staging by externally visible anatomy of the living fish. *Dev Dyn*. 2009;238(12):2975-3015. doi:10.1002/dvdy.22113
57. Arratia G, Schultze H-P. Reevaluation of the caudal skeleton of certain actinopterygian fishes: III. Salmonidae. Homologization of caudal skeletal structures. *J Morphol*. 1992;214(2):187-249. doi:10.1002/jmor.1052140209
58. Thieme P, Warth P, Moritz T. Development of the caudal-fin skeleton reveals multiple convergent fusions within Atherinomorpha. *Front Zool*. 2021;18(1):20. doi:10.1186/s12983-021-00408-x
59. Arratia G, Vila I, Lam N, Guerrero CJ, Quezada-Romegialli C. Morphological and taxonomic descriptions of a new genus and species of killifishes (Teleostei: Cyprinodontiformes) from the high Andes of northern Chile. *PLoS One*. 2017;12(8):e0181989. doi:10.1371/journal.pone.0181989
60. Costa WJEM. The caudal skeleton of extant and fossil cyprinodontiform fishes (Teleostei: Atherinomorpha): comparative morphology and delimitation of phylogenetic characters. *Vertebr Zool*. 2012;62(2):161-180.
61. Gaudant J. Découverte d'une nouvelle espèce de poissons cyprinodontiformes (*Prolebias delphinensis* nov. sp.) dans l'Oligocène du bassin de Montbrun-les-Bains (Drôme). *Geol Mediterr*. 1989;16:355-370. doi:10.3406/geolm.1989.1431
62. McDowall RM. The principal caudal fin ray count - a fundamental character in the galaxioid fishes. *N. Z. J. Zool*. 2001; 28(4):395-405. doi:10.1080/03014223.2001.9518278
63. Desvignes T, Robbins AE, Carey AZ, et al. Coordinated patterning of zebrafish caudal fin symmetry by a central and two peripheral organizers. *Dev Dyn*. 2022. doi:10.1002/dvdy.475
64. Mabee PM, Crotwell PL, Bird NC, Burke AC. Evolution of median fin modules in the axial skeleton of fishes. *J Exp Zool*. 2002;294(2):77-90. doi:10.1002/jez.10076
65. Wang L, Sun F, Wan ZY, et al. Genomic basis of striking fin shapes and colors in the fighting fish. *Mol Biol Evol*. 2021;38(8): 3383-3396. doi:10.1093/molbev/msab110
66. Rosen DE. The relationships and taxonomic position of the halfbeaks, killifishes, silversides, and their relatives. *Bull Am Mus Nat Hist*. 1964;127:217-267.
67. Gosline WA. Some osteological features of modern lower teleostean fishes. *Smithsonian Misc Collect*. 1961;142(3):1-42.
68. Parenti LR. A phylogenetic and biogeographic analysis of cyprinodontiform fishes (Teleostei, Atherinomorpha). *Bull Am Mus Nat Hist*. 1981;168:335-557.
69. Hollister G. Caudal skeleton of Bermuda shallow water fishes, 4, order Cyprinodontes: Cyprinodontidae, Poeciliidae. *Zool Sci Contrib N Y Zool Soc*. 1940;25(9):97-112.
70. De Pinna MCC. Teleostean monophyly. In: Stiassny MLJ, Parenti LR, Johnson GD, eds. *Interrelationships of Fishes*. San Diego: Academic Press; 1996:147-162.
71. Thieme P, Schnell NK, Parkinson K, Moritz T. Morphological characters in light of new molecular phylogenies: the caudal-fin skeleton of Ovalentaria. *Royal Society Open Science*. 2022; 9(1):211605. doi:10.1098/rsos.211605
72. Flammang BE, Alben S, Madden PGA, Lauder GV. Functional morphology of the fin rays of teleost fishes. *J Morphol*. 2013; 274(9):1044-1059. doi:10.1002/jmor.20161
73. Walker M, Kimmel C. A two-color acid-free cartilage and bone stain for zebrafish larvae. *Biotech Histochem*. 2007;82(1):23-28. doi:10.1080/10520290701333558

How to cite this article: Rees L, König D, Jaźwińska A. Platyfish bypass the constraint of the caudal fin ventral identity in teleosts. *Developmental Dynamics*. 2022;251(11):1862-1879. doi:10.1002/dvdy.518